LETTER

doi:10.1038/nature12127

Deep fracture fluids isolated in the crust since the Precambrian era

G. Holland[1,2], B. Sherwood Lollar[3], L. Li[3]†, G. Lacrampe-Couloume[3], G. F. Slater[4] & C. J. Ballentine[1]

Fluids trapped as inclusions within minerals can be billions of years old and preserve a record of the fluid chemistry and environment at the time of mineralization[1–3]. Aqueous fluids that have had a similar residence time at mineral interfaces and in fractures (fracture fluids) have not been previously identified. Expulsion of fracture fluids from basement systems with low connectivity occurs through deformation and fracturing of the brittle crust[4]. The fractal nature of this process must, at some scale, preserve pockets of interconnected fluid from the earliest crustal history. In one such system, 2.8 kilometres below the surface in a South African gold mine, extant chemoautotrophic microbes have been identified in fluids isolated from the photosphere on timescales of tens of millions of years[5]. Deep fracture fluids with similar chemistry have been found in a mine in the Timmins, Ontario, area of the Canadian Precambrian Shield. Here we show that excesses of ^{124}Xe, ^{126}Xe and ^{128}Xe in the Timmins mine fluids can be linked to xenon isotope changes in the ancient atmosphere[2] and used to calculate a minimum mean residence time for this fluid of about 1.5 billion years. Further evidence of an ancient fluid system is found in ^{129}Xe excesses that, owing to the absence of any identifiable mantle input, are probably sourced in sediments and extracted by fluid migration processes operating during or shortly after mineralization at around 2.64 billion years ago. We also provide closed-system radiogenic noble-gas (^{4}He, ^{21}Ne, ^{40}Ar, ^{136}Xe) residence times. Together, the different noble gases show that ancient pockets of water can survive the crustal fracturing process and remain in the crust for billions of years.

The Precambrian crystalline basement accounts for over 30% of the exposed surface area of the continents, yet the character, communication and residence times of fluids within it remain little explored. Crystalline basement fracture waters from the Canadian, Fennoscandian and South African continental cratons have recently drawn scientific attention because they possess concentrations of H_2 as high as 7 mM (ref. 6): that is, they are as rich in H_2 as the hydrothermal vents or ocean spreading centres[7]. This H_2 has been shown to be produced by radiolysis of water[8] and by serpentinization[9] and to provide the energy source for deep chemoautotrophic microbial ecosystems[5]. The Witwatersrand basin in South Africa is the most extensively studied among these crustal basement systems. There, radiogenic noble gases in the deepest fracture waters provide evidence for groundwater residence times of up to 25 million years (Myr)[5,10], indicating that this habitat has been isolated in the crystalline basement from the photosphere on geologic timescales. How prevalent and how ancient these fluid pockets might be remains unclear.

Here we report noble-gas isotopic compositions from some of the deepest bulk fracture fluids yet sampled from a working mine (Supplementary Videos). These fluids occur 2.4 km below the surface in crystalline rocks about 2.7 billion years (Gyr) in age, from the Precambrian Shield near Timmins, Ontario, Canada. The Timmins mine is a volcanogenic massive sulphide deposit producing copper and zinc ore[11]. Geologically, the Timmins site comprises a series of episodic volcanic eruptions intercalated with both terrigenous and marine sedimentary deposits formed in a shallow seafloor setting about 2.719–2.711 Gyr ago[12]. The deposit is relatively undeformed, metamorphosed to greenschist grade 2.67–2.69 Gyr ago[13], with a late metasomatic event at 2.64 Gyr (ref. 14). Exploration boreholes within the mine that produce water rich in hydrogen, methane, nitrogen and helium were sampled for stable and noble-gas isotope determination, following refs 5 and 15–17 (Methods). ^{3}He/^{4}He ratios vary between $0.0052R_a$ and $0.0153R_a$ (where R_a is the ^{3}He/^{4}He ratio in air, 1.4×10^{-6}) confirming that radiogenic helium accounts for more than 99% of the ^{3}He and ^{4}He (ref. 18). Ne isotope data indicate no significant mantle component (Fig. 1), but rather mixing between air-saturated water (ASW) and a distinctly different radiogenic end-member, consistent with elevated

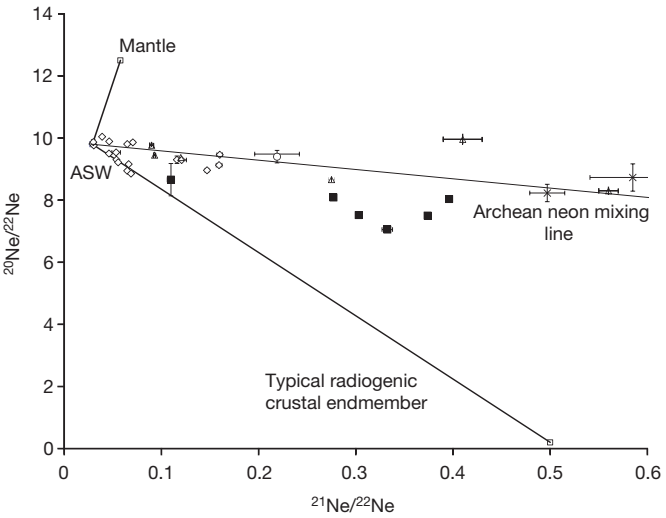

Figure 1 | Comparison of the Neon isotopic composition of free fluids and fluid inclusions in ancient crust. Data presented are: Timmins free fluids (solid squares, this work); Witwatersrand basin fracture waters (open diamonds) and fluid inclusions in bulk quartzite rock (open circle)[3]; fluid inclusions from vein quartz from the Kaapvaal craton, South Africa (crosses)[3]; CH_4-rich fluid inclusions from Yilgarn craton, Western Australia (open triangles)[1] and end-member compositions (mantle, ASW, Archean crust; and typical radiogenic crust). Nucleogenic Ne is generated by ^{17}O,^{18}O$(\alpha, n)^{20}$Ne, ^{21}Ne, ^{19}F$(\alpha, n)^{22}$Na(β^+) and ^{19}F$(\alpha, p)^{22}$Ne. Typical radiogenic continental environments have a ^{21}Ne/^{22}Ne lower than would be predicted by the O/F ratio alone due to preferential siting of F proximal to U (ref. 27) and have a typical ^{21}Ne/^{22}Ne value of around 0.47 at the ^{20}Ne/^{22}Ne zero intercept[18,27]. Ne isotope data from fluid inclusions in Archean terrains[1,3] are characterized by a significantly higher ^{21}Ne/^{22}Ne intercept of 3.3 ± 0.2 (ref. 3), consistent with the average crustal O/F ratio[18]. With the exception of sample 12287-1 (see Supplementary Information), the Timmins fluids indicate ASW mixing with an Archean Ne end-member and show no evidence for radiogenic contributions or input from outside this terrain. Error bars are as shown or are smaller than the plotted symbols and are 1σ.

[1]School of Earth, Atmospheric and Environmental Sciences, Manchester University, Manchester M13 9PL, UK. [2]Lancaster Environment Centre, Lancaster University, Lancaster LA1 4YQ, UK. [3]Department of Earth Sciences, University of Toronto, Ontario, M5S 3B1, Canada. [4]School of Geography and Geology, McMaster University, Hamilton, Ontario L8S 4K1, Canada. †Present address: Department of Earth and Atmospheric Sciences, University of Alberta, Edmonton T6G 2E3, Canada.

Table 1 | He, Ne and Ar isotope data of Timmins gas samples

Sample	$^{3}He/^{4}He$ (R_a)	Error	$^{20}Ne/^{22}Ne$	Error	$^{21}Ne/^{22}Ne$	Error	$^{40}Ar/^{36}Ar$	Error	$^{38}Ar/^{36}Ar$	Error
12261	0.0134	0.0033	7.501	0.0315	0.3739	0.0013	27173	446	0.1874	0.0005
12299-1	0.0133	0.0019	8.037	0.0657	0.3960	0.0035	44384	1554	0.1876	0.0005
12299-2	0.0153	0.0013	7.520	0.0554	0.3030	0.0032	28168	2050	0.1871	0.0004
12299-3	0.0147	0.0019	8.087	0.072	0.2770	0.0045	31787	2154	0.1875	0.0005
12287-1	0.0052	0.0012	8.660	0.5200	0.1098	0.0037	6564	123	0.1879	0.0006
12287-2	0.0113	0.0025	7.053	0.0623	0.3324	0.0054	24180	963	0.1879	0.0005

Errors quoted on all ratios are 1σ. $^{3}He/^{4}He$ are displayed relative to atmospheric ratio (R/R_a) = 1.4×10^{-6}.

$^{21}Ne/^{22}Ne$ previously identified in fluid inclusions in Archean terrains[1,3]. One extraordinary feature of the present study is that here the Archean Ne isotope signature has been discovered not in fluids trapped in inclusions, but in the radiogenic noble-gas-rich fracture fluids discharging from exploration boreholes, with water and gas flow rates of 0.1 to over 2 litres per minute (Supplementary Table 1). $^{40}Ar/^{36}Ar$ values in these samples (up to 44,384) are the highest yet reported in a free fluid (Table 1). High-precision Xe isotope data (Table 2) using multi-collector mass spectrometry[15] show isotopic excesses relative to modern atmosphere (denoted by asterisks) at all masses normalized to ^{130}Xe (Fig. 2). $^{131–136}Xe^*$ represent normal uranium fission and based on this we can rule out exotic nuclear processes or reaction routes for $^{129}Xe^*$. To our knowledge, these $^{129}Xe^*$ are the first excesses observed in a non-magmatic freely flowing fluid and show that an ancient fluid process signal has been preserved. $^{124–128}Xe^*$ appears to preserve an ancient atmosphere signal that allows a residence time to be estimated for these fluids.

The most intriguing component of the Xe mass spectra is the $^{124,126,128}Xe^*$ values (Fig. 2), indicating enrichment of the lightest isotopes of Xe. The Timmins fluids have ^{36}Ar concentrations in the original water phase similar to that of ASW (Methods) and $^{130}Xe/^{36}Ar$ ratios in excess of ASW (Supplementary Fig. 1). Xe enrichment is often inferred to be sediment-derived. However, the Xe-enriched component is not correlated with $^{124,126,128}Xe^*$, showing that the mass fractionation of $^{124–128/130}Xe$ is not derived from the sediment: a finding supported by recent experimental studies[19]. The $^{124,126,128}Xe^*$ must therefore be a primary feature of the atmosphere-derived component.

Extreme ultraviolet radiation and asteroid bombardment in the first few hundred million years of Earth's history have often been invoked to explain the preferential loss of the light isotopes of Xe in the Earth's atmosphere relative to those of other Solar System components[20]. Recently, evidence supporting ongoing, rather than early, Xe fractionation of the atmosphere throughout geological time has been derived from inclusions trapping ancient air in Archean barites and quartz grains[2,21]. The evolution of the Xe isotopes in Earth's atmosphere through this mechanism can be used to identify and date ancient water that has equilibrated with the early atmosphere (Fig. 3).

If the atmosphere evolved from an initial solar composition, as indicated by Kr isotopes[16,20], the average Timmins $^{124,126,128}Xe^*$ value is 26%–43% of that predicted by the Pujol model[2], assuming the fluids were trapped and preserved at the time of the last regional fluid event 2.64 Gyr ago. There are three explanations for this mismatch. The first is that the Pujol model has yet to be calibrated for this period and that the Timmins fluids do preserve 100% of the Xe signal of the atmosphere at this time in Earth's history—and in fact provide this calibration. The fracture fluids would then have to be 2.64 Gyr old. The second is that the Timmins fracture fluids could contain up to 74% modern Xe, and the $^{124,126,128}Xe^*$, in the context of the Pujol model, would then give a mean residence time for the fracture fluid of 1.5–1.85 Gyr (Fig. 3). Third, the accretionary Xe isotopic composition may have been chondritic and the observed $^{124,126,128}Xe^*$ would then be much closer to that expected for a 2.64-Gyr-old fluid (Fig. 3).

$^{129}Xe^*$ is also clearly resolved in the Timmins mine fluids. This could either be a magmatic signal[22] or the result of the decay of ^{129}I (half-life $t_{1/2}$ = 15.7 Myr). Production of ^{129}I in the crust by *in situ* ^{238}U, and more exotic radiogenic production routes of $^{129}Xe^*$, can be ruled out (Supplementary Information). We are then required to find a mantle or near-surface source of $^{129}Xe^*$. If the $^{129}Xe^*$ is mantle-derived, this should correlate with ^{3}He, the most unequivocal indicator of mantle input[17]. The absence of such a correlation and $^{3}He/^{129}Xe^*$ ratios in the fracture fluids ranging from 0.3 to 23, orders of magnitude lower than typical mantle values (about 500), requires extreme He/Xe elemental fractionation to preserve a Xe mantle signature without the corresponding He. We note that a mantle source for $^{129}Xe^*$ would also be associated with a $^{124}Xe^*$. However, mantle $^{129}Xe^*/^{124}Xe^*$ derived from the Bravo system[17] is 1.640 ± 209, which is an order of magnitude higher than we find in this work (199 ± 63). Therefore a mantle source for $^{129}Xe^*$ can account for only 12% ± 4% of the $^{124–128}Xe^*$ observed.

We can next consider cosmogenic ^{129}I, which is concentrated and deposited in carbon-rich sediments[23]. The periods of volcanic activity that formed the Timmins ore deposit were interspersed every few million years with carbonaceous sedimentary deposits, typically conglomerates, turbidites and greywackes[12,14] that were subsequently isolated from the surface by the next eruptive phase. This is a scenario that may have resulted in closed-system evolution of the $^{129}I–^{129}Xe$ system after each eruptive phase. Subsequent alteration of these trapped carbon-rich sediments produced the graphitic carbon observed in these sequences[24] and, critically, may have liberated substantial amounts of ^{129}I or ^{129}Xe. Using the average concentration of $^{129}Xe^*$ in our samples of 2.12×10^{9} atoms of $^{129}Xe^*$ per g H_2O, 10 m^3 of sediment would be

Table 2 | Xe isotope data of Timmins gas samples

Sample	$^{124}Xe/^{130}Xe$	Error	$^{126}Xe/^{130}Xe$	Error	$^{128}Xe/^{130}Xe$	Error	$^{129}Xe/^{130}Xe$	Error
12261	0.023762	164	0.022071	216	0.47528	057	6.5667	171
12299-1	0.023824	203	0.022101	177	0.47454	047	6.5710	066
12299-2	0.023724	130	0.022068	132	0.47545	048	6.5730	131
12299-3	0.023895	141	0.021976	116	0.47582	048	6.5664	092
12287-1	0.023613	026	0.021924	042	0.47365	019	6.5282	026
12287-2	0.023659	135	0.022196	171	0.47417	028	6.5823	132

Sample	$^{131}Xe/^{130}Xe$	Error	$^{132}Xe/^{130}Xe$	Error	$^{134}Xe/^{130}Xe$	Error	$^{136}Xe/^{130}Xe$	Error
12261	5.2342	115	6.8712	055	3.0002	018	2.7139	114
12299-1	5.2335	063	6.8460	068	2.9630	018	2.6634	027
12299-2	5.2475	115	6.7998	190	2.8941	012	2.5774	088
12299-3	5.2424	073	6.8268	150	2.9305	023	2.6234	068
12287-1	5.2263	026	6.6445	040	2.6272	005	2.2501	018
12287-2	5.2525	094	6.8186	095	2.9206	012	2.6073	099

Errors quoted on all ratios are last significant figures at 1σ.

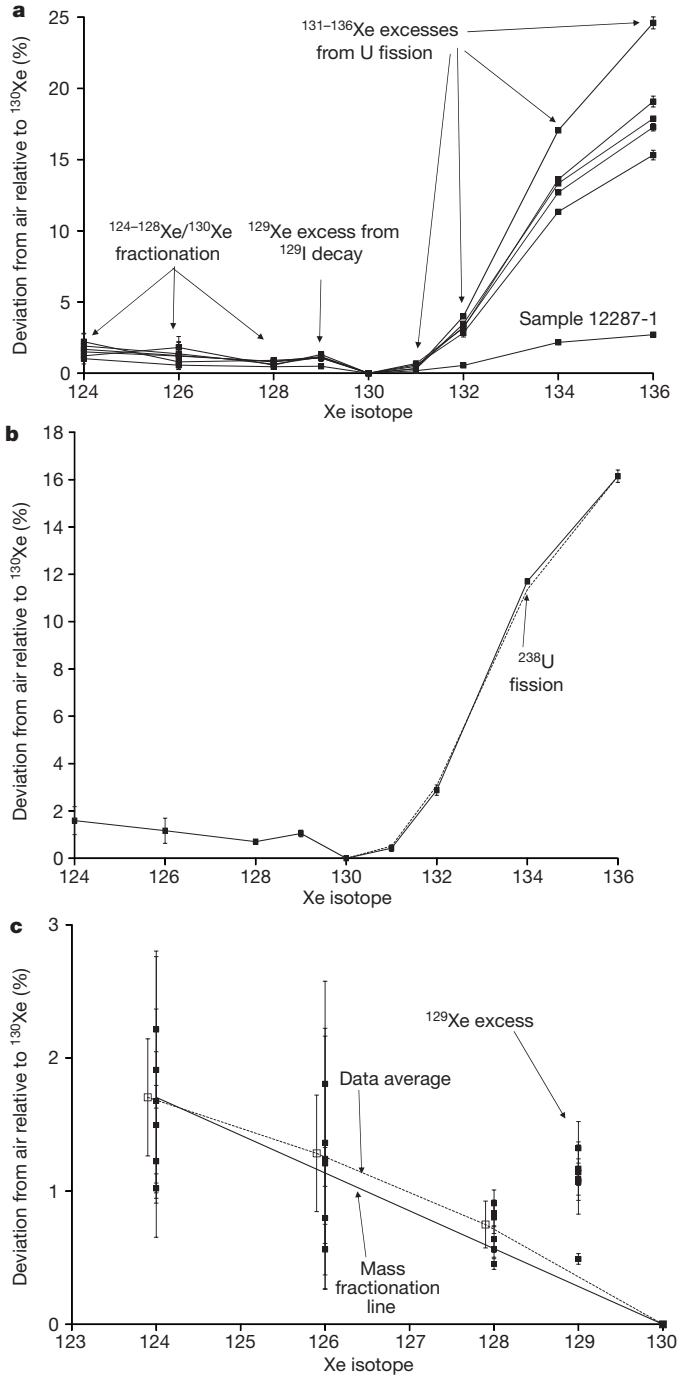

Figure 2 | Xenon isotopic spectrum. **a**, Isotopic ratios of Xe expressed as percentage deviation from air, relative to ^{130}Xe, shown for individual samples. Data show excess Xe (Xe*) at all masses. One sample (12287-1; see Table 1) has a much larger air-derived component. This is also observed in both Ne and Ar data (Table 1), probably indicating a small amount of air contamination (Supplementary Information). **b**, ^{131,132,134,136}Xe is a fission product from U. The data points show the average of all samples compared to ^{238}U fission spectrum (dashed lower line). The data are clearly within error of the ^{238}U fission spectrum and suggest that no other fission source significantly contributes to the heavy xenon isotope spectrum. **c**, ^{124,126,128,129}Xe* are observed in all samples. Individual samples (small solid squares) and averages of all samples except the air-contaminated sample 12287-1 are shown (open square). Errors are 1σ. Average ^{124,126,128}Xe* data (dashed line) are within error of the mass fractionation line (solid line). ^{129}Xe* in all samples is greater than the excess caused by mass fractionation, requiring either a cosmogenic ^{129}I or mantle ^{129}Xe source to explain most of the observed ^{129}Xe* and can only be reconciled with a fluid that has preserved this component since about 2.64 Gyr (see main text).

required to provide the ^{129}Xe* observed in the fracture fluids associated with 1 m^3 of Precambrian Shield rock. We note that these values are conservative and, as these processes are not well constrained, the amount of sediment required may be more than an order of magnitude less (Methods).

A sediment-derived source for the ^{129}Xe* might have been initiated by regional metamorphic events that resulted in reducing hydrothermal fluids known to have penetrated the basement between 2.69 and 2.64 Gyr ago[13,14]. Preservation of this signature in fracture fluids could only have occurred if these fluids were also from this time period. Magmatic activity, the source of any mantle-derived noble gases, also initiated around 2.79 Gyr ago and continued until around 2.64 Gyr ago[12,14]. The region has been quiescent since this period. Therefore, regardless of whether ^{129}Xe* was sediment- or mantle-derived, both hypotheses, importantly, require isolation of the sampled bulk fluids for time periods that extend over a significant period of Earth's existence.

The consequence of such an ancient isolation ought also to be seen in the radiogenic noble gases. There are two possible sources of the radiogenic noble gases in the fracture fluids: those produced *in situ* and those that are externally derived. Calculated *in situ* ages provide an important reference point (Methods). In this context the Ne isotope signature (Fig. 1) provides strong evidence that we do not have contributions to the radiogenic noble gases from anywhere other than the Archean terrain. Although it is not possible to rule out mechanisms that might concentrate radiogenic noble gases within portions of the Archean terrain, we make the a priori assumption that this is negligible to test our hypothesis of an ancient fluid. Using radionuclide U, Th and K concentrations for the local crystalline basement, we calculate the range of fluid residence times as averages of all samples (except for the air-contaminated sample 12287-1) to be 1,142 ± 645 Myr, 1,655 ± 789 Myr, 1,498 ± 784 Myr and 1,610 ± 825 Myr for ^{4}He,

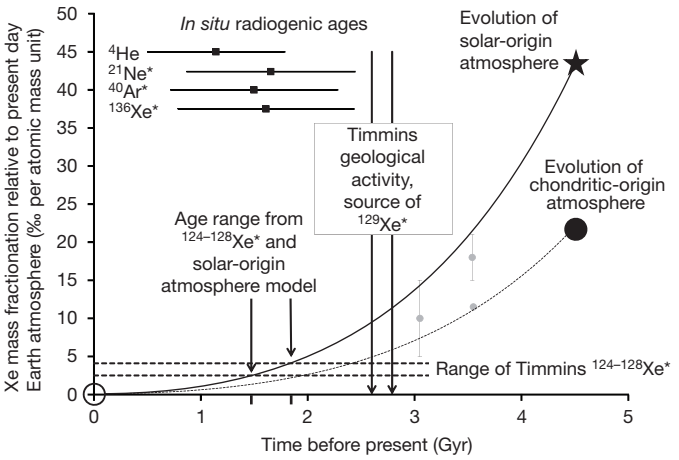

Figure 3 | The xenon isotopic evolution of Earth's atmosphere shown over time[2], relative to modern atmosphere. The chondritic, solar[28] and modern atmosphere values are shown as a solid circle, star and open circle, respectively. The solid curve is the evolution of the modern atmosphere from solar, which is our preferred initial composition[16]. The evolution of a chondritic-derived atmosphere is shown as a dashed curve. Grey data points are from refs 2, 21 and 29. The horizontal black dotted lines are the ±1σ range of the observed ^{124,126,128}Xe* of the Timmins samples (except the air-contaminated sample 12287-1), expressed per atomic mass unit (dalton). The vertical solid lines reflect the time period over which geological activity occurred at the Timmins site (approximately 2.7 to 2.64 Gyr). The solid black squares are *in situ* radiogenic noble gas ages for ^{4}He, ^{21}Ne, ^{40}Ar and ^{136}Xe, including errors; see Supplementary Table 3. Using a solar composition, the Timmins data require the Xe to have been isolated 1.5–1.85 Gyr ago (tick marks on *x* axis), or alternatively, account for 26–43% of the Xe now present if the ancient Xe component is indeed about 2.64 Gyr old. These are internally consistent with the range suggested by the ^{4}He, ^{21}Ne*, ^{40}Ar* and ^{136}Xe* residence times. Errors on radiogenic ages reflect one standard deviation of five samples and porosity variance (see Methods).

^{21}Ne, ^{40}Ar and ^{136}Xe respectively (see Supplementary Tables 1–3 and Methods). These are younger than 2.64 Gyr, but still exceptionally old and consistent with the range derived from the ^{124,126,128}Xe* and atmosphere evolution age (Fig. 3).

$^{124–128}$Xe*, ^{129}Xe* and radiogenic noble-gas *in situ* fracture fluid residence times (Supplementary Table 3) each provide independent evidence that the sampled fracture fluids have been isolated for at least a billion years, with a ^{129}Xe signature possibly preserved for as long as 2.64 Gyr. The discovery that ancient fluid environments capable of supporting life can remain isolated for hundreds of millions to billions of years may require changes in our understanding of the extent of the Earth's crust that may be habitable, and the part that such potential buried biomes play in preserving, evolving and propagating life on planetary timescales. Mars, like the Precambrian shields on Earth, is dominated by tectonically quiescent geologic terrains which are billions of years old, some with serpentinized ultramafic rocks capable of sustaining production of reduced gases such as found in the terrestrial Archean fracture fluids[25,26]. If such ancient fluids, with millimolar concentrations of H_2 and CH_4, are preserved deep in the terrestrial crust on billion-year timescales, perhaps similar potential buried biomes may be preserved at depth in the subsurface of Mars on planetary timescales.

METHODS SUMMARY

Sample collection. All samples were collected at the borehole collar. A packer was placed into the opening of the borehole and sealed to the inner rock walls below the water level to seal the borehole from the mine air and minimize air contamination, following the method of refs 15 and 30. Gas and water were allowed to flow through a gas–water sampling chamber (Supplementary Videos) long enough to displace any air remaining in the borehole or the apparatus before sampling. Plastic tubing was attached to the end of the packer and the flow of gas and/or water from the borehole was directed into a graduated sampling bucket. Temperature, pH and conductivity were measured on the outflowing water from the packer by respective field kits. Water flow was measured by filling the graduated sampling vessel three times. Gas flow was measured by filling the sampling vessel with water, then displacing a known volume of water from an inverted graduated funnel. For each borehole, gas flow rates were also measured three times and average values are reported. For noble-gas analysis, gas was collected in 60-cm-long, 10-mm-diameter, internally polished refrigeration-grade copper tubing sealed using the refrigeration clamping procedure outlined by ref. 31 or crimper cold welding. This technique of gas sampling and storage is well established and ensures there has been no noble-gas contamination or loss due to leakage or diffusion.

Full Methods and any associated references are available in the online version of the paper.

Received 31 July 2012; accepted 28 March 2013.

1. Kendrick, M. A., Honda, M., Walshe, J. & Petersen, K. Fluid sources and the role of abiogenic-CH_4 in Archean gold mineralization: constraints from noble gases and halogens. *Precambr. Res.* **189,** 313–327 (2011).
2. Pujol, M., Marty, B. & Burgess, R. Chondritic-like xenon trapped in Archean rocks: a possible signature of the ancient atmosphere. *Earth Planet. Sci. Lett.* **308,** 298–306 (2011).
3. Lippmann-Pipke, J. *et al.* Neon identifies two billion year old fluid component in Kaapvaal Craton. *Chem. Geol.* **283,** 287–296 (2011).
4. Sleep, N. H. & Zoback, M. D. Did earthquakes keep the early crust habitable? *Astrobiology* **7,** 1023–1032 (2007).
5. Lin, L.-H. *et al.* Long-term sustainability of a high-energy, low-diversity crustal biome. *Science* **314,** 479–482 (2006).
6. Sherwood Lollar, B. *et al.* Isotopic signatures of CH_4 and higher hydrocarbon gases from Precambrian Shield sites: a model for abiogenic polymerization of hydrocarbons. *Geochim. Cosmochim. Acta* **72,** 4778–4795 (2008).
7. Kelley, D. S. *et al.* A serpentinite-hosted ecosystem: the Lost City hydrothermal field. *Science* **307,** 1428–1434 (2005).
8. Lin, L.-H. *et al.* Radiolytic H_2 in continental crust: nuclear power for deep subsurface microbial communities. *Geochem. Geophys. Geosyst.* **6,** Q07003 (2005).
9. Sherwood Lollar, B. *et al.* Abiogenic methanogenesis in crystalline rocks. *Geochim. Cosmochim. Acta* **57,** 5087–5097 (1993).
10. Lippmann, J. *et al.* Dating ultra-deep mine waters with noble gases and ^{36}Cl, Witwatersrand Basin, South Africa. *Geochim. Cosmochim. Acta* **67,** 4597–4619 (2003).
11. Bleeker, W. & Parrish, R. R. Stratigraphy and U–Pb zircon geochronology of Kidd Creek: implications for the formation of giant volcanogenic massive sulphide deposits and the tectonic history of the Abitibi greenstone belt. *Can. J. Earth Sci.* **3,** 1213–1231 (1996).
12. Thurston, P. C. *et al.* Depositional gaps in Abitibi Greenstone Belt stratigraphy: a key to exploration for syngenetic mineralization. *Econ. Geol.* **103,** 1097–1134 (2008).
13. Thompson, P. H. A new metamorphic framework for gold exploration in the Timmins-Kirkland Lake area, western Abitibi greenstone belt: Discover Abitibi Initiative. *Ontario Geologic Survey Open-File Rep.* **6162,** 1–104 (2005).
14. Bleeker, W., Parrish, R. R. & Sager-Kinsman, A. in *The Giant Kidd Creek Volcanogenic Massive Sulfide Deposit, Western Abitibi Subprovince, Canada* (eds Hannington, M. D. & Barrie, C. T.) *Econ. Geol. Monogr.* **10,** 43–69 (1999).
15. Sherwood Lollar, B. *et al.* Abiogenic formation of gaseous alkanes in the Earth's crust as a minor source of global hydrocarbon reservoirs. *Nature* **416,** 522–524 (2002).
16. Holland, G., Cassidy, M. & Ballentine, C. J. Meteorite Kr in Earth's mantle suggests a late accretionary source for the atmosphere. *Science* **326,** 1522–1525 (2009).
17. Holland, G. & Ballentine, C. J. Seawater subduction controls the heavy noble gas composition of the mantle. *Nature* **441,** 186–191 (2006).
18. Ballentine, C. J. & Burnard, P. Production, release and transport of noble gases in the continental crust. *Rev. Mineral. Geochem.* **47,** 481–538 (2002).
19. Marrocchi, Y., Robert, F. & Marty, B. Adsorption of xenon ions onto defects in organic surfaces: implications for the origin and the nature of organics in primitive meteorites. *Geochim. Cosmochim. Acta* **75,** 6255–6266 (2011).
20. Pepin, R. O. On the origin and early evolution of terrestrial planet atmospheres and meteoritic volatiles. *Icarus* **92,** 2–79 (1991).
21. Pujol, M., Marty, B., Burnard, P. & Philipott, P. Xenon in Archean barite: weak decay of ^{130}Ba, mass-dependent isotopic fractionation and implication for barite formation. *Geochim. Cosmochim. Acta* **73,** 6834–6846 (2009).
22. Staudacher, T. Upper mantle origin for Harding County well gases. *Nature* **325,** 605–607 (1987).
23. Santos, F. J. *et al.* ^{129}I record in a sediment core from Tinto River (Spain). *Nucl. Instrum. Methods Phys. Res. B* **259,** 503–507 (2007).
24. Downes, M. J., Hodges, D. J. & Derwedumen, J. in *Gold '82: The Geology, Geochemistry and Genesis of Gold Deposits (Proc. Symp. "Gold '82". Univ. Zimbabwe, May 24–28, 1982)* (ed. Foster, R. P.) 435–448 (A. A. Balkema, 1984).
25. Mumma, M. J. *et al.* Strong release of methane on Mars in northern summer 2003. *Science* **323,** 1041–1045 (2009).
26. Ehlmann, B. L., Mustard, J. F. & Murchie, S. L. Geologic setting of serpentine-bearing rocks on Mars. *Geophys. Res. Lett.* **37,** L06201 (2010).
27. Kennedy, B. M., Hiyagon, H. & Reynolds, J. Crustal neon: a striking uniformity. *Earth Planet. Sci. Lett.* **98,** 277–286 (1990).
28. Wieler, R. & Baur, H. Krypton and xenon from the solar wind and solar energetic articles in two lunar ilmenites of different antiquity. *Meteoritics* **29,** 570–580 (1994).
29. Srinivasan, B. Barites: anomalous xenon from spallation and neutron-induced reactions. *Earth Planet. Sci. Lett.* **31,** 129–141 (1976).
30. Ward, J. A. *et al.* Microbial hydrocarbon gases in the Witswatersrand Basin, South Africa: implications for the deep biosphere. *Geochim. Cosmochim. Acta* **68,** 3239–3250 (2004).
31. Ballentine, C. J. &. Sherwood Lollar, B. Regional groundwater focusing of nitrogen and noble gases into the Hugoton-Panhandle giant gas field, USA. *Geochim. Cosmochim. Acta* **66,** 2483–2497 (2002).

Supplementary Information is available in the online version of the paper.

Acknowledgements We thank S. Shirey for discussion on the geological history of the study areas and P. Burnard for a review. This work was funded by NSERC Discovery and CRC grants to B.S.L., a UK-NERC grant to C.J.B. and Deep Carbon Observatory support to C.J.B. and B.S.L. We are indebted to P. Calloway, P. Jurenovski, A. Marcotte and L. Kieser for assistance in sample collection.

Author Contributions G.H., B.S.L. and C.J.B. designed the project, interpreted the data and wrote the paper. G.H. analysed the samples. G.F.S. and L.L. collected the field samples. G.F.S., L.L. and G.L.-C. characterized the gas and water samples and provided critical comment and input on the manuscript.

Author Information Reprints and permissions information is available at www.nature.com/reprints. The authors declare no competing financial interests. Readers are welcome to comment on the online version of the paper. Correspondence and requests for materials should be addressed to C.J.B. (chris.ballentine@manchester.ac.uk).

METHODS

Sample collection. All samples were collected at the borehole collar. A packer was placed into the opening of the borehole and sealed to the inner rock walls below the water level to seal the borehole from the mine air and minimize air contamination, following the method of refs 15 and 30. Gas and water were allowed to flow through a gas–water sampling chamber (Supplementary Videos) long enough to displace any air remaining in the borehole or the apparatus before sampling. Plastic tubing was attached to the end of the packer and the flow of gas and/or water from the borehole was directed into a graduated sampling bucket. Temperature, pH and conductivity were measured on the outflowing water from the packer by respective field kits. Water flow was measured by filling the graduated sampling vessel three times. Gas flow was measured by filling the sampling vessel with water, then displacing a known volume of water from an inverted graduated funnel. For each borehole, gas flow rates were also measured three times and average values are reported. For noble-gas analysis, gas was collected in 60-cm-long, 10-mm-diameter, internally polished refrigeration-grade copper tubing sealed with the refrigeration clamping procedure outlined by ref. 31 or crimper cold welding. This technique of gas sampling and storage is well established and ensures there has been no noble-gas contamination or loss due to leakage or diffusion.

^{129}I analytical method. Samples for ^{129}I analysis were filtered through 0.2-μm filters and 1-litre pre-cleaned Nalgene bottles were completely filled, leaving no head space. The bottles were then wrapped in aluminium foil and maintained in a 4 °C cold room before ^{129}I determination by accelerator mass spectrometry. Iodine in the sample was chemically reduced to iodide. 2 mg of potassium iodide carrier with known ^{129}I concentration—$^{129}I/^{127}I = (2.2 \pm 04) \times 10^{-14}$—were added to the sample and the iodide was oxidized to molecular iodine by addition of sodium nitrite. The iodine was extracted into hexane and then back-extracted into a sodium bisulphite/sulphuric acid solution. Silver nitrate was added to ensure complete precipitation of the analyte as silver iodide. The dried silver iodide sample was mixed with an equal weight of 350-mesh niobium powder and pressed into stainless steel sample holders for analysis by accelerator mass spectrometry at the University of Toronto IsoTrace Facility. The sample data are normalized to IsoTrace Reference Material 2, which has been calibrated to NIST-3230 I and II standards to have $^{129}I/^{127}I = (1.313 \pm 0.017) \times 10^{-11}$. The blank (potassium iodide carrier added to de-ionized water) for this procedure is typically $(0.075 \pm 0.010) \times 10^8$ atoms per litre and the standard deviation (1σ) ranges from 5% to 10%.

Atmosphere-derived noble gases and produced water. The dominant source of atmosphere-derived noble gas isotopes in subsurface fluids is from air dissolved in groundwater (ASW) (see review[32]). Oil and gas fields in contact with ancient basinal brines often show excesses of $^{84}Kr/^{36}Ar$ and $^{130}Xe/^{36}Ar$ relative to the values found in ASW. This has been attributed to sediment-derived contributions of air-derived Kr and Xe that are sorbed onto carbonaceous-rich sediments and transferred to the fluid phase through water-rock interaction. Similarly, although they are less well understood, excess $^{20}Ne/^{36}Ar$ relative to ASW are also often found in old crustal fluids[33–35]. We use here ocean water at 10 °C as our reference ASW, containing 1.47×10^{-7} cm^3 of ^{20}Ne, 1.01×10^{-6} cm^3 of ^{36}Ar, 3.99×10^{-8} cm^3 of ^{84}Kr and 5.2×10^{-10} cm^3 of ^{130}Xe (at standard temperature and pressure, STP) per gram of H_2O (ref. 36).

All samples in this study also show excess $^{20}Ne/^{36}Ar$, $^{84}Kr/^{36}Ar$ and $^{130}Xe/^{36}Ar$ relative to ASW. A coherent increase in these values is most simply attributed to mixing between ASW and a fluid enriched in ^{20}Ne, ^{84}Kr and ^{130}Xe relative to ^{36}Ar (Supplementary Fig. 1). Importantly, there is no coherent behaviour of the radiogenic noble-gas ratios ($^4He/^{40}Ar^*$, $^{21}Ne^*/^{40}Ar^*$ and $^{136}Xe^*/^{40}Ar^*$, where the isotopic values in excess of air and denoted by the asterisk are ascribed to radiogenic sources with the atmosphere-derived noble-gas elemental ratios. From this we conclude that the ASW noble-gas patterns (Supplementary Fig. 1) must represent heterogeneity of the air-derived noble gases, incorporated into the fluids as production proceeds *in situ*, rather than an artefact of phase separation during production and sampling.

Gases are naturally exsolving from the flowing fracture waters. Gas/water volume ratios of 0.045 to 0.72 g of H_2O per cm^3 of gas (at STP) will result in near-complete transfer of any noble gases in the groundwater into the gas phase, according to Henry's Law. The concentration of the noble gases in the gas phase and the gas/water ratio is used to calculate the original concentration of the noble gases in the groundwater before exsolution. Using this method, groundwater ^{36}Ar concentrations are calculated to range between 2.23×10^{-7} and 2.46×10^{-6} cm^3 (at STP) per gram of H_2O, with a modal value of about 8.5×10^{-7} cm^3 (at STP) per gram of H_2O. Neglecting sample 12287-1, with its anomalously low $^{40}Ar/^{36}Ar$ ratio suggesting some degree of air contamination, the average value of this sample suite is 9.04×10^{-7} cm^3 (at STP) per gram of H_2O and is within 9% of the reference ASW value. The similarity of the integrated *in situ* groundwater ^{36}Ar concentration with that of ASW suggests that the groundwater has undergone little, if any, open-system phase separation since last equilibrating with the atmosphere.

Radiogenic noble-gas concentrations. The variance of $^4He/^{36}Ar$ ratios in the samples is smaller than that of the water/gas ratio variability between boreholes (Supplementary Table 1). To remove the effect of sample-to-sample variance caused by differences in gas/water flow rates between boreholes, we take the average measured value (neglecting the air-contaminated sample 12287-1) of 9.04×10^{-7} cm^3 (at STP) per gram of H_2O and use the observed $^4He/^{36}Ar$ to calculate the ^{4}He concentration in the same water. Neglecting sample 12287-1 again, ^{4}He concentrations in the *in situ* groundwater range from 0.086 to 0.204 cm^3 (at STP) per gram of H_2O (with an average of 0.136 cm^3 (at STP) per gram of H_2O). We note that any gas phase not in solution, whether under hydrostatic or lithostatic pressure, occupies negligible volume compared to the relatively incompressible water phase. At 1.0% porosity (ref. 37) and a density of 2.7 g cm^{-3}, 1 g of rock will contain 0.0037 g formation water and 5.62×10^{-4} cm^3 (at STP) ^{4}He and 1.15×10^{-4} cm^3 (at STP) $^{40}Ar^*$. A similar calculation is made for $^{21}Ne^*$ and $^{136}Xe^*$.

Porosity range. The porosity of the basement rocks hosting the sampled fluids nevertheless represents an uncertainty in deriving the bulk-rock radiogenic noble-gas content. Bucher and Stober[37] report a characteristic porosity for basement rocks of 1.0%. Well tests give flow effective porosities in the Black Forest basement of 0.1% to 2.1% (ref. 38), with a corresponding range of low hydraulic conductivities for tests on rocks from the Canadian Shield[39]. Reported porosity ranges in granite are similar and range between 0.3% and 1.0% (ref. 40) and 0.9% and 2.3% (ref. 41). In gneiss the data are more limited, but the Urach test site in Germany reports a fracture porosity of 0.1%–0.5% (ref. 42). We adopt the value of 1.0% from ref. 37 and assign a 1σ uncertainty to this of ±0.45% to include the observed porosity range at a 2σ level of confidence.

External versus internal sources of radiogenic gases. There are two possible sources of the radiogenic noble gases in the fracture fluids: those produced *in situ* and those that are externally derived. Within basinal sedimentary aquifers, for example, a significant additional source is derived from the deeper crust and accumulates beneath the aquitard[43]. The mechanism of transfer of noble gases from the crystalline basement to shallow regions is uncertain, with evidence for episodic, advective[44] and fault-controlled[45] mechanisms as well as uniform continual input[43,46]. While the contribution of external sources of radiogenic noble gases cannot be ruled out, the limits of the '*in situ*' noble-gas ages must be recognized and additional evidence for their validity acquired. This might be the geological context or data, such as presented here, on xenon light-isotope deviations from atmosphere and ^{129}Xe excess values that support ancient sedimentary sources and processes.

***In situ* fluid residence time.** *In situ* ^{4}He and ^{40}Ar production rates can be calculated using:

$$^4He = 8 \times [^{238}U] \times (e^{\lambda_{238} t} - 1) + 7 \times [^{235}U] \times (e^{\lambda_{235} t} - 1) + 6 \times [^{232}Th] \times (e^{\lambda_{232} t} - 1) \quad (1)$$

and

$$^{40}Ar = 0.105 \times [^{40}K] \times (e^{\lambda_{40} t} - 1) \quad (2)$$

where ^{4}He and ^{40}Ar are the radiogenic noble-gas concentrations that would be produced within a rock in time t, containing $[^{238}U]$, $[^{235}U]$, $[^{232}Th]$ and $[^{40}K]$ concentrations respectively. λ_{238}, λ_{235}, λ_{232} and λ_{40} are the decay constants for the respective radio-isotopes and the value 0.105 is the fraction of ^{40}K that decays to ^{40}Ar. $^{21}Ne^*$ and $^{136}Xe^*$ are produced in proportion to radiogenic helium with $^4He/^{21}Ne^*$ and $^4He/^{136}Xe^*$ production ratios of 9.96×10^6 and 3.033×10^8 respectively[18]. Observed $^4He/^{21}Ne^*$ in this study's samples are between 0.54 and 0.97 (average, 0.725) of the crustal production ratio, whereas observed $^4He/^{136}Xe^*$ are 0.54–0.936 (average, 0.743) of the crustal production ratio. The $^{21}Ne^*/^{136}Xe^*$ ratios are between 0.769 and 1.14 (average, 0.975) of the crustal production ratio. We note that it seems that the ^{4}He concentration is approximately 30% lower than that expected from the $^{21}Ne^*$ and $^{136}Xe^*$. The $^{21}Ne^*/^{136}Xe^*$ values are within the expected production range and the small variance from sample to sample in all radiogenic ratios provides further evidence that there are no significant artefacts caused by degassing kinetics or phase fractionation during gas production or sampling.

The resolved radiogenic $^4He/^{40}Ar^*$ ratio in all samples ranges from 3.99 to 5.36 (average, 4.68). This is a very small range and falls between the predicted ratios of 6.56 and 3.55 for production at 0 Gyr and 2.67 Gyr ago respectively within the Kidd-Munro group, probably representing the average composition of the parent elements (Th = 9 parts per million (p.p.m.), U = 2 p.p.m. and K = 2%; ref. 47). We also consider the regional values for the southwest Abitibi belt (Th = 4.31 p.p.m., U = 0.91 p.p.m. and K = 1.48%; ref. 48), from which we calculate $^4He/^{40}Ar^*$ ratios of 4.14 and 2.24 for 0 and 2.67 Gyr ago, respectively. We note that there is better agreement between predicted and measured $^4He/^{40}Ar^*$ using Kidd-Munro-group

concentrations of parent elements and therefore provide *in situ* ages in the manuscript using these values. Because Kidd-Munro-group parent-nuclide concentrations are higher than other compositions (for example, southwest Abitibi Belt), *in situ* residence times presented here are a conservative estimate yielding lower limits for the ages. Using equations (1) and (2) and the radio-element concentrations for the Kidd-Munro group, we calculate ^{4}He accumulation ages of 1.14×10^{9} years and ^{40}Ar accumulation ages of 1.50×10^{9} years, respectively (Supplementary Table 3). This method assumes all release coefficients $\lambda_{He,Ne,Ar,Xe} = 1$, which is consistent with the observed radiogenic ^{4}He/^{21}Ne*/^{40}Ar*/^{136}Xe* at or close to the predicted production ratios and again yields lower *in situ* age limits.

Calculating ^{129}Xe* concentrations. Measured radiogenic ^{129}Xe* concentrations in the six individual samples range from $1.09–3.2 \times 10^{-11}$ cm^3 of ^{129}Xe* per cm^3 of gas. As with radiogenic noble gases, we assume the co-produced water is completely degassed but originally contained ^{36}Ar with near-ASW concentrations of 9.04×10^{-7} cm^3 (at STP) per gram of H_2O. ^{130}Xe concentration in fracture water is therefore derived from observed ^{130}Xe/^{36}Ar and ASW ^{36}Ar concentration. Once ^{130}Xe concentration is obtained, ^{129}Xe* is calculated from the increase in ^{129}Xe/^{130}Xe over the value in air. Multiplying these values by $(6.02 \times 10^{23}/22{,}400)$ converts these initial concentrations in the fracture fluid to atoms per gram of H_2O. Undegassed samples therefore contain $1.24–3.61 \times 10^{9}$ atoms ^{129}Xe* per gram of H_2O, with an average of 2.85×10^{9} atoms of ^{129}Xe* per gram of H_2O. Correcting for the mass fractionation observed in $^{124–128}$Xe/^{130}Xe for each sample reduces this to $(0.90–2.70) \times 10^{9}$ atoms of ^{129}Xe* per gram of H_2O, with an average of 2.12×10^{9} atoms of ^{129}Xe* per gram of H_2O.

***In situ* production routes for ^{129}Xe*.** *In situ* ^{238}U production of ^{129}I in the crust typically reaches a steady state after about 80 Myr in crystalline basement hosted waters[49]. The ^{129}I concentration in sample 12299-2, determined by AMS, is 1.23×10^{8} atoms per litre. At steady state this would require 5.48×10^{11} years to produce the observed 2.12×10^{12} atoms of ^{129}Xe* per litre of H_2O. Given that this is greater than the age of the Universe, this allows us to discount *in situ* ^{238}U-derived ^{129}I as a significant source of the ^{129}Xe*. Radiogenic sources of ^{129}Xe, such as epithermal or thermal neutron capture by tellurium, or chemically fractionated fission products from natural reactors, all produce significant and distinct quantities of heavy Xe isotopes[18]. However, the $^{131–136}$Xe/^{130}Xe pattern is indistinguishable from simple ^{238}U fission (Fig. 2b), and these exotic production routes can also be discounted.

Calculation of cosmogenic ^{129}I contribution from sediment. Cosmic-ray spallation of xenon in the atmosphere produces an equilibrium cosmogenic ^{129}I concentration today of about 2×10^{9} atoms per litre in sediment porewater[50]. This is three orders of magnitude too low to account for the observed ^{129}Xe*. Nevertheless, iodine is sequestered by organic sediments, with pre-nuclear fallout sediment cores documented with ^{129}I concentrations of 1×10^{6} atoms per gram of sediment (ref. 23). We assess here whether the iodine concentration in the sediments associated with the Timmins mineralizing system is sufficient to generate the ^{129}Xe* observed in the Timmins mine fluid samples. Assuming $1\% \pm 0.45\%$ porosity, 1 m^3 of rock would contain $10{,}000 \pm 4{,}500$ g of H_2O in fluid fractures. Assuming total degassing of water, the average ^{129}Xe* from six measured boreholes is 2.12×10^{9} atoms of ^{129}Xe* per g of H_2O. Based on this, 1 m^3 of Precambrian Shield contains $2.12 \times 10^{9} \times (10{,}000 \pm 4{,}500\,\text{g}) = (2.12 \pm 0.95) \times 10^{13}$ atoms of ^{129}Xe*. Overlying sediment containing 1×10^{6} atoms per gram of ^{129}I and a density of 2 g cm^{-3} will produce 2×10^{12} atoms of ^{129}Xe* per m^3. Approximately 10 m^3 of sediment is therefore required to supply the ^{129}Xe* observed in the fracture fluids associated with 1 m^3 of Precambrian Shield rock. This mechanism requires 100% efficient mobilization of iodine (if mobilization occurs before ^{129}I decay) and xenon (if mobilization occurs after ^{129}I decay), and retention of all iodine (or xenon) during compaction and dewatering.

However, we note that there is significant uncertainty in these calculations: (1) Ref. 51 reports an ^{129}I concentration of 1.4×10^{7} atoms per gram of marine sediments: an order of magnitude higher than used in the calculation above. (2) The elevated ^{124}Xe/^{130}Xe observed in these samples, if it is an indication of a less fractionated ancient atmosphere, would require 30% more xenon to have been present in the atmosphere at the time of formation[20], generating enhanced production of ^{129}I. (3) The ultraviolet flux penetrating the anoxic Archean atmosphere was considerably higher[52]. (4) The intensity of ultraviolet radiation was likely to have been greater from the younger Sun[53]. These factors may combine to reduce the amount of sediment required by more than two orders of magnitude from 10 m^3 to less than 0.1 m^3 for each 1 m^3 of 1% porosity rock.

Geological setting. The stratiform massive base metal sulphide (Cu–Zn) deposits of the Timmins mine lie on the western end of the Abitibi greenstone province of the Canadian Shield[12,14]. The area is characterized by steeply dipping Archean felsic, mafic and ultramafic deposits interlayered with metasedimentary deposits referred to as the Kidd-Munro assemblage. Deposition began with massive felsic rhyolite and rhyolitic volcanoclastic rocks extruded onto ancient sea bed deposits (ultramafics) in a proximal seafloor setting. The volcanoclastic deposits appear to be from brecciation and resedimentation of a previously consolidated rhyolite unit. Within these units are flow-banded subvolcanic sills and dike intrusions of massive rhyolite and metavolcanoclastic rhyolites[54]. Stringer ore is closely associated with the upper section of the felsic piles, probably forming as a result of silica-rich and metal-rich hydrothermal fluids circulating just below the sea floor. Banded and massive sulphide ores overlie the stringer zones, deposited on the volcanics as precipitate where hydrothermal solutions rich in metals entered the sea water[54]. Discontinuous carbonaceous horizons ranging from argillite to chert occur within the volcanoclastics, are closely associated with the zones of ore deposition, and are believed to represent periods of quiet chemical sedimentation intervals of 2–27 Myr between periods of episodic volcanism[12]. The deposit is relatively undeformed, metamorphosed to greenschist grade between 2.67 to 2.69 Gyr, with a late metasomatic event at 2.64 Gyr (refs 12 and 14).

32. Schwarzenbach, R. P., Gschwend, P. M. & Imboden, D. M. *Environmental Organic Chemistry* (John Wiley and Sons, 1993).
33. Torgersen, T. & Kennedy, B. M. Air-Xe enrichments in Elk Hills oil field gases : role of water in migration and storage. *Earth Planet. Sci. Lett.* **167,** 239–253 (1999).
34. Torgersen, T., Kennedy, B. M. & van Soest, M. C. Diffusive separation of noble gases and noble gas abundance patterns in sedimentary rocks. *Earth Planet. Sci. Lett.* **226,** 477–489 (2004).
35. Zhou, Z., Ballentine, C. J., Schoell, M. & Stevens, S. H. Identifying and quantifying natural CO_2 sequestration processes over geological timescales: the Jackson Dome CO_2 deposit, USA. *Geochim. Cosmochim. Acta* **86,** 257–275 (2012).
36. Kipfer, R., Aeschbach-Hertig, W., Peeters, F. & Stute, M. in *Noble Gases in Geochemistry and Cosmochemistry* (eds Porcelli, D, Ballentine, C. J. & Wieler, R.) *Rev. Mineral. Geochem.* **47,** 615–700 (2002).
37. Bucher, K. & Stober, I. Fluids in the upper continental crust. *Geofluids* **10,** 241–253 (2010).
38. Stober, I. Permeabilities and chemical properties of water in crystalline rocks of the Black Forest, Germany. *Aquat. Geochem.* **3,** 43–60 (1997).
39. Stober, I. & Bucher, K. Hydraulic properties of the crystalline basement. *Hydrogeol. J.* **15,** 213–224 (2007).
40. Guillot, L. *et al.* Porosity changes in a granite close to quarry faces: quantification and distribution by ^{14}C-MMA and Hg porosimetries. *Eur. Phys. J. A* **9,** 137–146 (2000).
41. Aquilina, L., de Dreuzy, J. R., Bour, O. & Davy, P. Porosity and fluid velocities in the upper continental crust (2 to 4 km) inferred from injection tests at the Soultz-sous-Forêts geothermal site. *Geochim. Cosmochim. Acta* **68,** 2405–2415 (2004).
42. Stober, I. & Bucher, K. in *Hydrogeology of Crystalline Rocks* (eds Stober, I. & Bucher, K.) 53–78 (Kluwer, 2000).
43. Torgersen, T. & Clarke, W. B. Helium accumulation in groundwater I: an evaluation of sources and the continental flux of crustal ^{4}He in the Great Artesian Basin, Australia. *Geochim. Cosmochim. Acta* **49,** 1211–1218 (1985).
44. Ballentine, C. J., O'Nions, R. K., Oxburgh, E. R., Horvath, F. & Deak, J. Rare gas constraints on hydrocarbon accumulation, crustal degassing and groundwater flow in the Pannonian Basin. *Earth Planet. Sci. Lett.* **105,** 229–246 (1991).
45. Kulongoski, J. T., Hilton, D. R. & Izbicki, J. A. Helium isotope studies in the Mojave Desert, California: Implications for groundwater chronology and regional seismicity. *Chem. Geol.* **202,** 95–113 (2003).
46. Bethke, C. M., Zhao, X. & Torgersen, T. Groundwater flow and the He-4 distribution in the Great Artesian Basin of Australia. *J. Geophys. Res. Solid Earth* **104,** 12999–13011 (1999).
47. Ketchum, J. W. F. *et al.* Pericontinental Crustal Growth of the Southwestern Abitibi Subprovince, Canada—U-Pb, Hf, and Nd Isotope Evidence. *Econ. Geol.* **103,** 1151–1184 (2008).
48. Moulton, B. J. A. *et al.* Archean subqueous high-silica rhyolite coulees: examples from the Kidd-Munro Assemblage in the Abitibi Subprovince. *Precambr. Res.* **189,** 389–403 (2011).
49. Bottomley, D. J., Renaud, R., Kotzer, T. & Clark, I. D. Iodine-129 constraints on residence times of deep marine brines in the Canadian Shield. *Geology* **30,** 587–590 (2002).
50. Martin, J. B., Gieskes, J. M., Torres, M. & Kastner, M. Bromine and iodine in Peru margin sediments and pore fluids: implications for fluid origins. *Geochim. Cosmochim. Acta* **57,** 4377–4389 (1993).
51. Price, N. B. & Calvert, S. E. The geochemistry of iodine in oxidised and reduced Recent marine sediments. *Geochim. Cosmochim. Acta* **37,** 2149–2158 (1973).
52. Farquhar, J., Bao, H. M. & Thiemens, M. Atmospheric influence of Earth's earliest sulfur cycle. *Science* **289,** 756–758 (2000).
53. Ribas, I. *et al.* Evolution of the solar activity over time and effects on planetary atmospheres. II. κ^1 Ceti, an analog of the Sun when life arose on Earth. *Astrophys. J.* **714,** 384–395 (2010).
54. Walker, R. R., Matulich, A., Amos, A. C., Watkins, J. J. & Mannard, G. W. The geology of the Kidd Creek mine. *Econ. Geol.* **70,** 80–89 (1975).